ACS Sustainable Chemistry & Engineering

pubs.acs.org/journal/ascecg

Research Article

Coupling of Flavonoid Initiation Sites with Monolignols Studied by Density Functional Theory

Laura Berstis, Thomas Elder, Richard Dixon, Michael Crowley,* and Gregg T. Beckham*

Cite This: https://dx.doi.org/10.1021/acssuschemeng.0c04240

Read Online

ACCESS | Metrics & More | Article Recommendations | Supporting Information

ABSTRACT: Lignin recalcitrance presents a challenge for the development of a bioeconomy that employs lignocellulosic feedstocks. The efficiency of lignin deconstruction is improved by a reduction of molecular weight, and given the discovery that flavones serve as initiation sites in lignin biosynthesis, these molecular weight reductions could potentially be achieved with plant metabolic engineering to over-express flavonoids. Upon increasing the flavonoid content in lignin, the bond strengths and properties of flavonoid-monolignol linkages become increasingly important. To that end, the current work applies density functional theory calculations to elucidate the bond dissociation enthalpies (BDEs) of flavonoid-monolignol linkages, including dimers with oxidized monolignols. Specifically, the dimer bond strengths and monomer hydrogen abstraction energies for the flavonoids tricin, chrysoeriol, luteolin, apigenin, catechin, epicatechin, epigallocatechin, and epigallocatechin gallate are calculated, when coupled to seven natural and engineered monolignols. Results indicate that 4′-O-β linkage strengths between flavonoids and monolignols are of comparable strength to inter-monolignol β-O-4 linkages, with average flavonoid-monolignol BDEs of 70.7 kcal/mol relative to ∼69.3 kcal/mol in analogous canonical monolignols. Epigallocatechin yielded the lowest 4′-O-β bond strength of 52.3 kcal/mol when coupled to an oxidized monolignol, while the flavones overall produced lower average BDEs, relative to the flavanols. Substituents at the 3′-C and 5′-C positions on flavonoids affected the dimer linkage strengths to a greater extent than glycosylation or substituents further from the linkage. *Erythro* and *threo* stereochemistry across the flavonoid-monolignol linkage library exhibited only small energetic differences and no pronounced correlations. Taken together, the predictions from this work support the concept that higher concentrations of flavonoid initiation sites in lignin may afford linkage properties conducive to more facile lignin depolymerization.

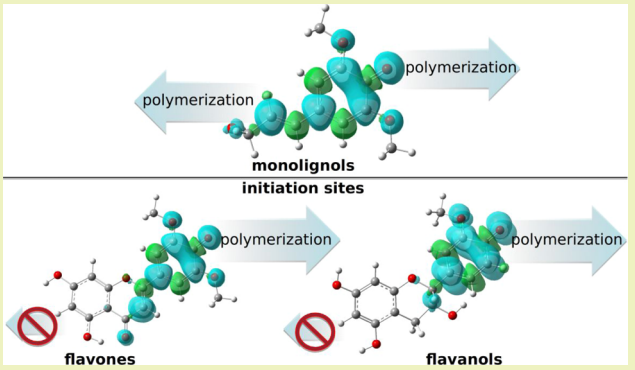

KEYWORDS: *lignin valorization, flavonoids, flavones, flavanols, tricin, catechin, epicatechin, bond dissociation enthalpy*

INTRODUCTION

As the energy and material demands of humankind continue to grow, lignocellulosic materials offer an increasingly attractive source of sustainable carbon-based feedstocks,[1,2] but the realization of a biobased economy will hinge upon the ability to valorize the plant biopolymer, lignin, alongside polysaccharides.[2−7] Lignin biosynthesis involves the polymerization of several phenylpropanoid monomers, most commonly, coniferyl, sinapyl, and *p*-coumaryl alcohols, which, respectively, generate guaiacyl (G), syringyl (S), and hydroxyphenyl (H) units in lignin. These monolignols polymerize by radical coupling reactions to form a diverse array of linkages due to several reactive sites of the delocalized radical in the monolignol. The β-O-4 bond is the most prevalent and constitutes 35−85% of intermonolignol linkages, depending on the plant type,[8] followed by β−β, 5-O-4, and β-5 linkages, among others.[9] This radical coupling chemistry of diverse monolignols forms a heterogeneous and recalcitrant polymer due to the lack of structural and chemical uniformity.[8,10−13]

Beyond the three canonical monolignols, new monomers and linkages that can incorporate into lignin of specific plant tissues and species are actively being discovered.[14−22] This ever-expanding spectrum of monomers found in nature importantly depicts the plasticity of lignin to accommodate chemical and structural modifications while preserving its native, protective function in plants.[15]

As the variability and malleability of lignin biosynthetic pathways become better understood, they enable the strategic engineering of less recalcitrant feedstocks.[23−26] The natural C-lignin polymer, for example, forms a linear homopolymer of caffeyl alcohol,[16,27] which challenges the conventional view of

Received: June 8, 2020
Revised: December 13, 2020

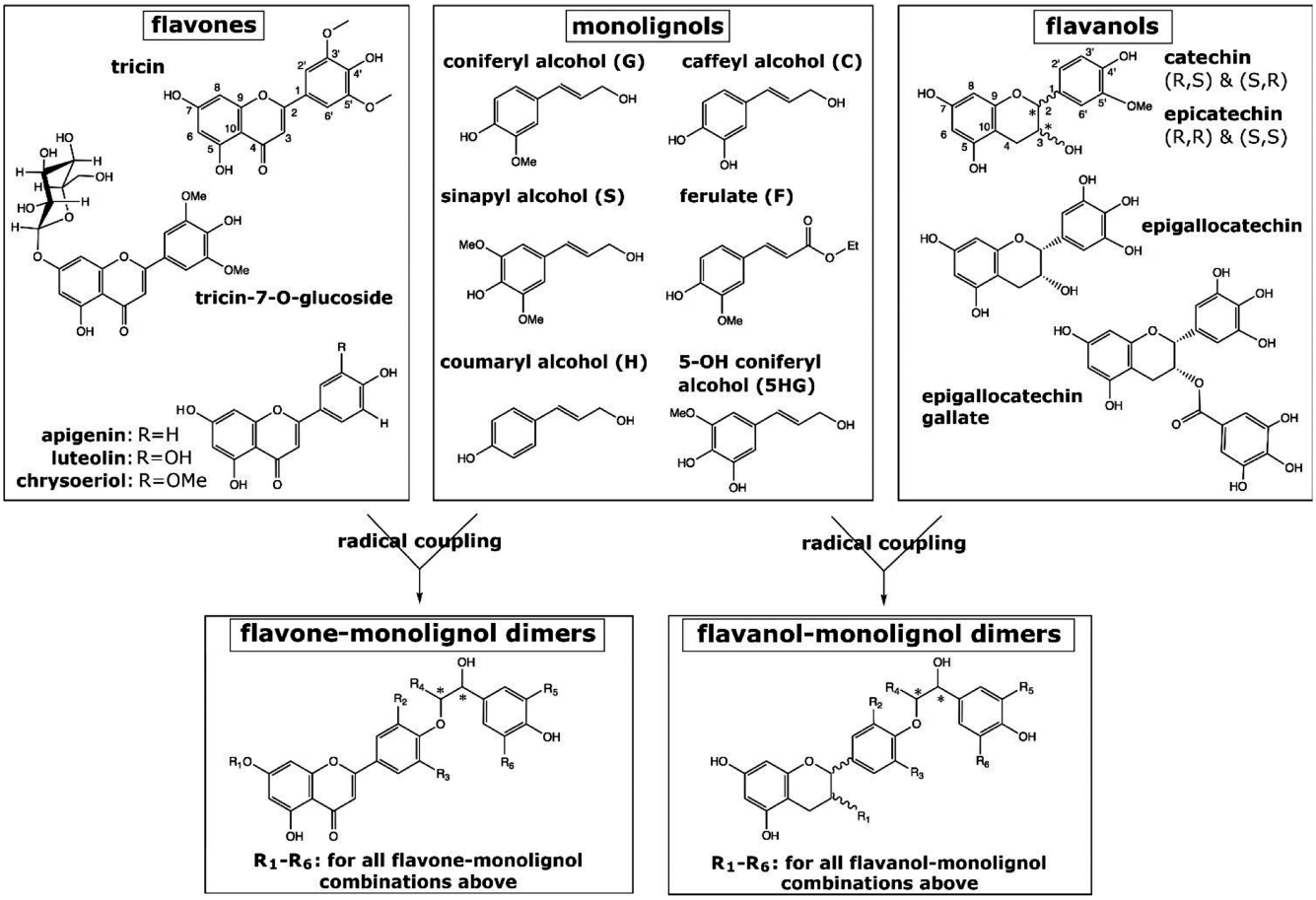

Figure 1. Coupling scheme of flavones and flavanols with coniferyl, caffeyl, sinapyl, feruloyl, coumaryl, and 5-hydroxyconiferyl monolignols into 4′-O-β linked flavonoid-monolignol dimers.

lignin as heterogeneous with chemically diverse linkages. Nearly homogeneous polymers were also achieved with F5H overexpression, yielding a more linear, S-enriched lignin,[28] and conversely, the F5H knock-out producing a polymer devoid of the S content.[25] By introducing a non-native feruloyl-CoA monolignol transferase gene, bioengineering efforts successfully introduced the oxidized monolignol ferulate, achieving more labile ester linkages in ZIP-lignin.[15,29,30] Taking engineered biosynthesis a step further, curcumin incorporation was recently reported in *Arabidopsis* lignin, which like ferulate facilitated depolymerization via a labile linkage.[21,31] Additional studies have furthermore demonstrated that even canonical monolignols are nonessential in lignin synthesis,[32] permitting considerable liberties in the engineering of novel lignin compositions.

Another approach to reduce biomass recalcitrance is to reduce the degree of polymerization of lignin, in light of experimental findings that lower molecular weight lignin polymers are more easily depolymerized.[33−36] A common approach in polymer science to reduce the molecular weight is to increase the concentration of initiation sites, producing more numerous shorter polymers. Recent discoveries in lignin biosynthesis have revealed the role of flavonoid molecules as chain initiators in lignin polymerization.[35,37−40] Several classes of flavonoids, including flavones and flavanols, have been of longstanding interest in medicine due to their antioxidant properties. The flavone tricin has been found to act as a highly effective radical scavenger and therefore received significant attention in the pharmaceutical industry as an anti-inflammatory and chemopreventative.[41,42] Likewise, the flavanols, catechin and epicatechin, are active against oxidative damage[43] and also studied in pharmaceutical sciences for their health benefits.[44−46] Inherently, this radical scavenging activity makes flavonoids suitable participants in radical recombination reactions of lignin biosynthesis. Analogous to monolignols, flavonoids can be deprotonated at the 4′-OH position,[10,47] generating a free radical that combines with activated monolignols.[16,27] Flavonoids have been observed across many species of plants and constitute an estimated 1.5%[39] or up to 8%[40] of the lignin content. A variety of glycosylated tricins have also been documented in plants, most commonly with glycosylation of the 7-OH and 5-OH groups.[40,48] The significance and function of diverse flavonoid types and glycosylation patterns remain to be clarified, yet it is stipulated that differences in the flavonoids impart distinct biological functions. For instance, tricin-glycoside concentrations are notably higher in alfalfa, halfa, and rice plant leaves,[40] exhibiting species- and tissue-specific trends. Further, the expression of different flavonoids is modulated in response to environmental conditions, demonstrated by a decrease in flavone glycoside levels seen in barley upon organic fertilization treatments.[49] Although flavonoids clearly play a key role in plant lignification, an investigation is still required to understand the properties of flavonoid-monolignol linkages. An improved understanding of initiation site−lignin interactions could facilitate the design of feedstocks that over-

https://dx.doi.org/10.1021/acssuschemeng.0c04240
ACS Sustainable Chem. Eng. XXXX, XXX, XXX−XXX

express specific flavonoids to regulate the lignin molecular weight.

Introducing higher concentrations of initiation sites in lignin with the goal of recalcitrance reduction makes the chemical nature of flavonoid-lignin linkages increasingly important. The corresponding bond strengths would need to remain tractably low, such that flavonoid-rich lignin would not come at a higher energetic cost to depolymerize. Put into context of transition state theory, a mere 1.36 kcal/mol increase in the activation energy of a bond-breaking chemical reaction results in a 10-fold decrease in the reaction rate, as may be seen by considering the expression

$$k \propto e^{-E_a/k_B T} \quad (1)$$

Accordingly, even subtle shifts in bond strengths can have significant outcomes in energy requirements and reaction efficiency. Furthermore, the design of lignin polymerization strategies would broadly benefit from understanding the electronic structure of native flavonoid-lignin linkages. The present work therefore evaluates the strength and electronic properties of the 4′-O-β linkages to lignin. Computational studies have contributed insights into the strengths of cleavable bonds in model lignin dimers by means of evaluating relative energetics and bond dissociation enthalpies (BDEs).[47,50−56] The same approaches can be applied to evaluate the 4′-O-β bond formation and cleavage energetics in flavonoid-monolignol dimers. The present work uses density functional theory (DFT) calculations to calculate the BDEs and properties of flavonoid-monolignol dimers for the flavones, tricin, apigenin, luteolin, and chrysoeriol (members of the tricin biosynthetic pathway,[57] which differ in their 3′ and 5′ substituents), and the flavanols, catechin, epicatechin, epigallocatechin, and epigallocatechin gallate, coupled with the monolignols: H, G, S, caffeyl (C), and 5-hydroxyconiferyl (5HG) alcohols and ferulate (Figure 1). The latter non-canonical monolignols have been demonstrated to reduce lignin chemical complexity and could perhaps be of an additive benefit to depolymerization efficiency, if paired with low-molecular-weight oligomers.

In addition to the flavonoid-monolignol 4′-O-β strengths, we calculate the hydrogen abstraction energy required for monomer activation during biosynthesis and the radical delocalization patterns. With these evaluations, we aim to (1) compare the relative BDEs of flavones and flavanols coupled to monolignols, (2) predict the reactivity of the radical monomers in coupling reactions, (3) evaluate the magnitude of substituent effects on dimer and monomer properties, and (4) examine stereochemical and geometric differences in the flavonoid-monolignol dimers. With this information, we consider what implications a higher prevalence of flavonoid-monolignol linkages may have for lignin depolymerization.

METHODS

All monomer and dimer geometries were initially prepared in Gaussian09[58] with a preliminary optimization using B3LYP/6-31G(d). Vibrational analyses confirmed that the structures were local minima, which were then used as starting points for conformational searches. The large number of rotatable bonds makes the conformer search a key step, given that the dimer conformation can affect the BDE prediction. Less stable, high-energy dimers could result in underestimated bond strengths, given the smaller ΔE between a higher-energy dimer and radical products. Therefore, a conformer library was generated for all monomer and dimer systems using the software TINKER,[59] in which a hopping algorithm perturbs geometries to search the conformational space for minima. In TINKER, the Merck Molecular Force Field (MMFF94)[60] was used for sampling conformer energies. Structures were saved if their energies satisfied a 10 kcal/mol cutoff from the lowest energy structure found, which resulted in a pool of several thousand conformers for each dimer system. While there are no guarantees of locating the global minimum in this conformational search method, this approach has been nevertheless found to sufficiently identify low-energy conformers, proving useful for comparing across diverse dimer bond energies.[27,47,50,54,61] After ranking the MMFF energies of the conformer pool, the 500 lowest energy structures were selected for optimization with the semiempirical method PM6 using Mopac.[62] The 20 most stable conformers from the semiempirical refinement were then optimized with DFT using unrestricted M06-2X/Def2-TZVPP with an ultrafine grid in Gaussian09. Unrestricted DFT was used to calculate the monolignol and flavonoid radical species as well as the singlet species for consistency. Vibrational analyses at 298.15 K were performed on all resulting systems to confirm that the structures were positive definite minimum geometries and to obtain the zero-point energy correction and thermochemistry of each species.

The M06-2X functional was chosen for the thermodynamic calculations, given that benchmarking works have demonstrated its robust predictivity for thermochemical properties,[63,64] which led to its application in many previous studies on lignin dimers.[27,50,55,56,61] This functional captures 94% of dispersion forces[63] and medium-range stacking interactions[65] and is therefore expected to achieve favorable accuracy for flavonoid-lignin dimers that can involve these intramolecular forces. The well-polarized triple-ζ Def2-TZVPP basis set has been shown to perform well for calculations of unpaired electrons[66] and provides sufficient basis functions for an accurate description of bond properties and interactions.

As with β-O-4 monolignol linkages, 4′-O-β flavonoid-monolignol linkages can form a racemic mixture of *erythro* stereochemistry (*R*,*S* or *S*,*R*) and *threo* stereochemistry (*R*,*R* or *S*,*S*).[14] Noted also in previous works,[27,61] the enantiomers within each type generate redundant energetics, with differences arising only from the inherent accuracy of the methods. Therefore, only one representative member of each the *erythro* and *threo* groups studied here was modeled, arbitrarily choosing the (*S*,*R*) and (*S*,*S*) dimer isomers. Within the flavanols, both stereocenter configurations were evaluated, including the catechin (*R*,*S* and *S*,*R*) and epicatechin (*R*,*R* and *S*,*S*) isomers. In contrast, dimers of flavonoids with ferulate subsequently condense into a double bond between C-α and C-β and thus have no 4′-O-β stereochemistry in the final product. However, for more direct comparison to the other monolignols, which remain saturated at these carbon centers, both the unsaturated and saturated, chiral feruloyl dimers were modeled in either stereochemistry.

Two methods of evaluating bond dissociation products were considered. In the first, the enthalpy of each radical dissociation product was determined with a single-point frequency calculation, frozen in the optimized geometry of the dimer. This "coordinate bond energy" evaluates the strength of the bond directly as it exists in the lowest energy dimer conformation. The second approach permits the reorganization of the radical products, which accounts for a rapid electronic and geometric relaxation upon bond cleavage. This latter approach is applied by Sangha,[53] as well in our previous bond strength computations in C-lignin[27] and 5-OH coniferyl alcohol.[61] In this method, no conformational search is performed on the radical products to avoid large-scale alterations relative to the dimer, which could result in the misrepresentation of bond strengths. Instead, only one downhill energy trajectory is followed in the optimization of each radical to the nearest local minimum. BDE predictions including this reorganization energy are expectedly lower due to the increased stability of the radical enthalpies. While this relaxed BDE evaluation may be more predictive for depolymerization at moderate to higher temperatures, both approaches are compared for additional insights into linkage strength trends, independent of instantaneous rearrangements.

https://dx.doi.org/10.1021/acssuschemeng.0c04240
ACS Sustainable Chem. Eng. XXXX, XXX, XXX−XXX

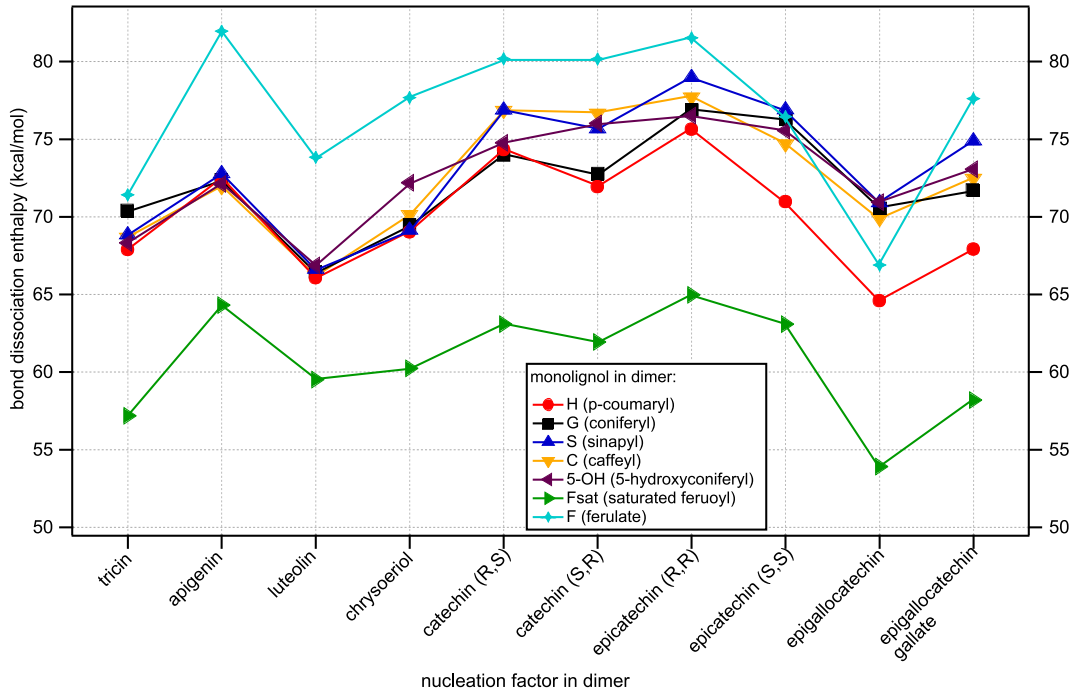

Figure 2. BDE of each flavonoid coupled to monolignols, where each marker presents the average BDE of the *threo* and *erythro* stereochemistry for each dimer. All BDE values of *threo* and *erythro* isomers are presented in Table S1.

RESULTS AND DISCUSSION

Flavonoid-Monolignol 4′-O-β BDEs. BDEs of the 4′-O-β flavonoid-monolignol dimer linkages resulting from optimized product geometries are presented in Figure 2 for stereoisomer averages, with all *threo* and *erythro* values tabulated in Table S1. The overall range of flavonoid-monolignol 4′-O-β bond strengths is slightly wider but comparable to the BDEs previously calculated for lignin dimers. For example, G−G dimers yielded an average of 68.8 kcal/mol among all stereoisomers and 68.7 for 5HG-G dimers,[71] 69.3 kcal/mol across the canonical monolignols H, G, and S,[81] and a range of 63.6−71.4 kcal/mol across all β-O-4 linkages of homodimers and heterodimers coupled with caffeyl alcohol.[27]

Most prominently observed in these data, the average BDE of any flavonoid coupled to saturated ferulate, F_{sat}, was 10.3 kcal/mol lower, relative to the nonoxidized monolignols. The average of these labile flavonoid-F_{sat} linkages was 61.9 kcal/mol, with the overall lowest BDE of 53.9 kcal/mol observed for the epigallocatechin-F_{sat} dimer (52.3 and 55.5 kcal/mol for the *erythro* and *threo* isomers, respectively), followed by tricin-F_{sat} (57.2 kcal/mol), and the epigallocatechin gallate-F_{sat} dimer (58.2 kcal/mol). In contrast, when including an unsaturated Cα−Cβ bond in the dimer with ferulate, the BDE consistently increases. Given this unique chemical difference of the unsaturated Cα-Cβ, the increase in 4′-O-β bond strength to the sp^2 carbon is logical, compared to the longer, more labile bond in the saturated model system. It is important to note, however, that the increased 4′-O-β linkage strength does not impact the ester bond present in ferulate and epigallocatechin gallate, which is easily hydrolyzed and imparts the reduced recalcitrance of ferulate-rich lignin.[82] The marked effect of oxidation adjacent to the linkage is, however, pronounced across all monolignol-flavonoid dimers. To further explore the impact of oxidation on 4′-O-β bond strength, the coupling of tricin to α-oxidized sinapyl was compared to the coupling with sinapyl alcohol, an α-hydroxyl-feruloyl model, and the model saturated F_{sat} compound (Figure 3). Sinapyl oxidation resulted

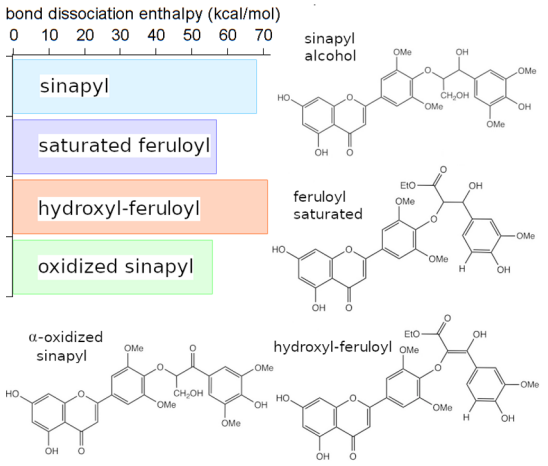

Figure 3. Comparison of BDE of tricin dimerized to (A) sinapyl alcohol, (B) F_{sat} (saturated feruloyl monolignol), (C) α-hydroxyl-ferulate, and (D) oxidized α-sinapyl alcohol.

in a 19% decrease of BDE to 56.0 kcal/mol, weakening the linkage to an even lower BDE than the F_{sat}-tricin dimer. Experimental efforts have previously demonstrated that oxidation of the α-hydroxyl group enhances depolymerization of intermonolignol linkages.[67,68] Our findings here show that a significant bond weakening is similarly achieved in flavonoid-monolignol linkages that involve an oxidized monolignol. Interestingly, as observed by the differences in bond strengths between ferulate and the model system F_{sat}, oxidation of either carbon adjacent to the 4′-O-β linkage does not appear to directly correlate with a reduction of the C−O bond strength, calling for a better exploration of the role of α- and β-oxidation in affecting lignin linkage strengths.

https://dx.doi.org/10.1021/acssuschemeng.0c04240
ACS Sustainable Chem. Eng. XXXX, XXX, XXX−XXX

Although the epigallocatechin-F_{sat} dimer yielded the lowest bond strength, the flavone bond strengths were consistently lower than flavanols, with an average across all flavone-monolignol dimers of 67.9 kcal/mol. For epigallocatechins (with and without gallate), this average rose to 69.8 kcal/mol, and finally, the highest average of 73.5 kcal/mol in (epi)-catechin-monolignol dimers. Unlike the flavanols, the flavones are characterized by an additional carbon−carbon double bond and carbonyl group, which effectively extend the conjugated π-system from the phenol-prime ring. The increased conjugation in flavones has greater capability to delocalize the unpaired electron density upon homolytic cleavage. Among the flavanols considered, chemical differences arise from the presence of the 3′- and 5′-OH groups in the epigallocatechins, in contrast to the 3′-H and 5′-OMe in the (epi)catechins. In epigallocatechins, not only do these hydroxyl substituents flanking the 4′-OH group involved in the linkage result in lower BDEs for this type of flavanol, but also these moieties could result in the formation of benzodioxane linkages,[17,27] which is discussed later.

Epigallocatechin gallate dimer bond strengths increased relative to epigallocatechin, with an average rise of 6.1 kcal/mol for all epigallocatechin gallate−monolignol pairs (Table S2). Despite the introduction of the conjugated gallate moiety, it lacks contiguous conjugation with the phenyl-prime ring, which would be needed to stabilize the products of homolytic cleavage. As seen in the monomer spin density calculations in the section entitled Monomer Hydroxyl BDEs, the radical does not delocalize onto the gallate ring, explaining the absence of a stabilizing effect. Further, the epigallocatechin gallate dimers were found to adopt folded structures, involving hydrogen bonds between hydroxyl groups, as well as aromatic stacking interactions. These interactions further lower the dimer enthalpy and accordingly increase the energy gap between the dimer and radical monomer products of bond cleavage. On account of the labile ester moiety between gallate and epigallocatechin, this flavanol is an attractive candidate for lignin engineering[35,69] and has been already demonstrated to improve the delignification and fermentability of structural saccharides.[44] Importantly, epigallocatechin gallate has two chemically similar 4′OH groups available to form linkages with monolignols and accordingly would no longer behave as a unidirectional initiation site but rather as a noncanonical monolignol. Nevertheless, the labile ester moiety present may further facilitate depolymerization reactivity via susceptibility to hydrolysis under mild reaction conditions.[83]

Substituent effects were examined on the flavone systems by comparing tricin (in which 3′ and 5′ methoxyl groups flank the 4′-O-β bond) to chrysoeriol, luteolin, and apigenin, wherein the 3′ and 5′ substituents are exchanged for hydroxyl groups or hydrogen (Figure 1). The most labile 4′-O-β linkages among the flavone-monolignol dimers were found for luteolin (65.3 kcal/mol), followed by tricin (67.4 kcal/mol), when averaging across the monolignols. The hydroxyl group in luteolin and the two methoxyl groups in tricin *ortho* to the 4′-O-β bond are therefore interpreted to reduce BDEs and indicate that electron-rich substituents can slightly weaken the linkage. The methoxyl and hydroxyl groups impart *ortho* inductive and mesomeric effects on the flavonoid phenyl ring that may be responsible for stabilizing the products of homolytic cleavage. This is consistent with observations of significantly changed NMR chemical shifts due to methoxyl and hydroxyl substituents on the phenyl-prime ring.[70] In contrast, the substituent modifications further from the flavonoid-monolignol linkage—whether on the monolignol phenol or glycosylation on the flavonoid—had a lesser effect on the linkage strength. Glycosylation at the 7-OH position on tricin, for example, only reduced the BDE from 70.4 to 68.4 kcal/mol (Table 1).

Table 1. BDE of Coniferyl Alcohol Dimerized to Tricin vs Tricin-7-O-Glc with Either Frozen or Relaxed Radical Product Geometries in kcal/mol

	dimer			
	G-(*S*,*R*)-tricin		G-(*S*,*R*)-tricin-7-O-Glc	
	(*S*,*R*)	(*S*,*S*)	(*S*,*R*)	(*S*,*S*)
bond coordinate BDE	94	94.5	84.9	95.7
relaxed BDE	70	70.7	65.6	71.2

Comparing the two BDE approaches, the bond coordinate energy predictions resulted in the anticipated higher enthalpies than the relaxed radical products, as seen by the average 21.7 kcal/mol above those calculated from the reorganized radicals (Table S1). The fact that the radical products underwent only a small geometric change in the local optimization following homolytic cleavage highlights the strong sensitivity of BDE evaluations to geometry. The most predominant trends nevertheless remain consistent between the evaluation types, particularly supporting the predominant finding of weaker F_{sat}-flavonoid linkages. While the bond coordinate energies possibly represent an upper limit of bond strength under conditions preventing rapid molecular rearrangement, the relaxed BDEs including reorganization energy better model the reactivity under conditions of higher temperature thermochemical processing and were therefore used as the basis for analyses in the remainder of this discussion.

4′-O-β Linkage Stereochemistry. Stereochemical effects were explored by comparing the relative enthalpies of dimer stereoisomers, $\Delta H(threo-erythro)$, presented in Table 2.

Table 2. $\Delta H(Threo-Erythro)$ in kcal/mol for the ZPE-Corrected Enthalpy of the Lowest Energy Conformers of Each Flavonoid-Monolignol Dimer

nucleation factor	monolignols					
	coumaryl alcohol	caffeyl alcohol	5HG alcohol	coniferyl alcohol	feruloyl, saturated	sinapyl alcohol
tricin	3.45	4.03	6.46	0.77	-1.92	0.41
apigenin	-0.26	-2.58	-3.48	-3.06	-1.71	-2.34
luteolin	-0.54	0.24	0.64	0.17	1.28	-0.83
chrysoeriol	1.25	-1.26	2.12	-6.16	-1.74	-2.95
catechin (R,S)	4.18	-0.17	-1.39	-0.02	0.88	2.89
catechin (S,R)	7.02	3.16	1.46	2.33	-1.09	0.00
epicatechin (R,R)	2.19	1.66	2.47	1.14	-4.10	1.51
epicatechin (S,S)	-11.52	2.73	0.75	0.97	-3.46	2.23
epigallocatechin	-1.35	5.85	6.56	7.10	3.19	6.64
epigallocatechin gallate	0.01	5.55	4.27	11.79	-2.52	5.87
	weaker threo linkage stronger erythro linkage				weaker erythro linkage stronger threo linkage	
ΔBDE(threo-erythro)	< -6.0	-6 - -3	-3 - 0	0 - 3	3 - 6	> 6.0

Similar to the findings for monolignols in previous works,[27,47,50,54] the flavonoid-monolignol enthalpies slightly varied between isomers, which in turn affected the dimer linkage strengths. However, isomer stability was found to only weakly correlate with the ΔBDE, as shown in Figure S1.

Although a subtle chemical difference, the cause of stereoisomer energy inequalities can be seen in the Neumann

https://dx.doi.org/10.1021/acssuschemeng.0c04240
ACS Sustainable Chem. Eng. XXXX, XXX, XXX−XXX

projections as viewed down the Cβ−Cα bond, as exemplified in Figure 4A for coniferyl alcohol coupled to epigallocatechin.

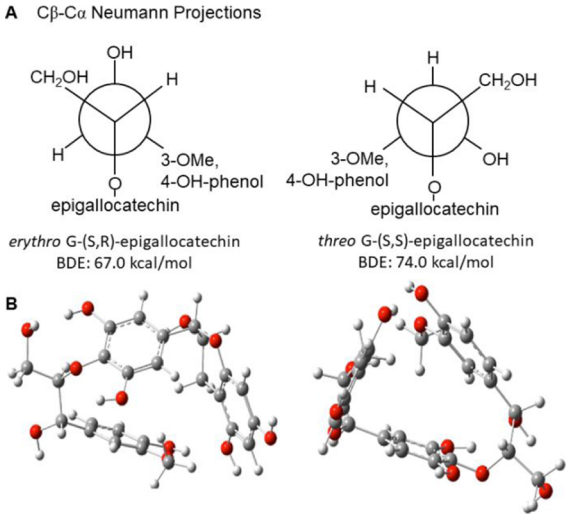

Figure 4. Neumann projections as viewed down the Cβ−Cα of the monolignol (A) and lowest energy conformers (B) for the *erythro* vs *threo* epigallocatechin-coniferyl alcohol dimer.

The *erythro* and *threo* stereochemical arrangements result in the intercalation of different substituents, such that the isomers experience unique steric stresses and can minimize into significantly different geometries (Figure 4B).

The average *erythro* dimer enthalpy was a negligible 0.55 kcal/mol lower than the average *threo* isomer enthalpy and the majority of stereoisomers had less than 2 kcal/mol difference in stability. This energy difference is of comparable magnitude with methodological accuracy, leading to the conclusion that neither global energetic preferences nor linkage strengths correlate with flavonoid-monolignol stereochemistry.

Dimer Structures and Interactions. The lowest energy dimers could generally be categorized as either extended, linear conformations or folded, globular conformations. A simple metric to assess dimer compactness was employed, namely, the distance between the aromatic 4-carbon on lignin and flavonoid 1′-carbon, as depicted in Table 3. In extended dimer geometries, this distance reaches a maximum of ∼9.4 Å and shortened to ∼4 Å in the folded conformations. In the folded geometries, this interplanar distance between conjugated rings and their off-center parallel plane orientations was characteristic of stacking interactions, or specifically, polar/π interactions between electron-rich aromatic rings.[72,73] The average C1′−C4 radius in flavones was 7.21 Å, versus 4.88 Å for flavanols, indicating the higher propensity of flavanol dimers to adopt folded conformations. Partly influencing these geometric preferences is the greater rigidity of the flavones due to their planar, conjugated structures. In contrast, the sp^3 hybridization on C2 and C3 of flavanols adds flexibility to fold and accommodate intramolecular interactions.

Table 3. Average Distances (in Å) between the Monolignol C4 and Flavonoid C1′ Atoms, with Example Folded and Extended Conformers

	coupled to flavones			coupled to flavanols		
monolignol	*erythro*	*threo*	isomer avg.	*erythro*	*threo*	isomer avg.
coumaryl	7.87	6.85	7.36	4.59	5.08	4.39
caffeyl	7.78	6.57	7.17	4.35	4.44	4.39
5HG	8.28	6.33	7.3	4.39	4.4	4.4
coniferyl	5.14	7.61	6.37	4.95	5.17	5.06
sinapyl	6.4	5.28	5.84	4.38	5.19	4.79
saturated feruloyl	9.41	9.02	9.21	5.48	6.08	5.78
ferulate	--		7.25	--		6.37

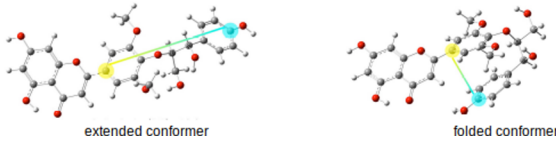

While small in comparison with the covalent linkages, hydrogen bonding and aromatic interactions affect the enthalpies of lignin oligomers and have been shown in experiments to substantially contribute to the self-assembly properties of lignin.[74−76] The full extent of noncovalent interactions is not captured in small dimer models, but these weak interactions warrant further investigations. The present DFT study did not include solvent models, which can lead to overestimated formation of noncovalent interactions that would otherwise be interacting with solvent molecules. Noncovalent interactions are nevertheless expected to arise in the presence of solvent and become increasingly relevant in more complex oligomers. Future works with MM/MD approaches recently parameterized for lignin[77] would be capable of robustly examining structure reactivity and quantify the extent to which specific intra- and intermolecular interactions affect oligomer properties.

Monomer Hydroxyl BDEs. Activation of the flavonoids is believed to proceed by the same mechanism of hydrogen abstraction as with monolignols, creating a pool of reactive radical monomers.[38] The BDE predictions of the 4′-OH of flavonoids and 4-OH of monolignols, shown in Table 4, reveal the broad range of hydroxyl bond strengths, from 78.5 to 87.0 kcal/mol, and a similar ∼10 kcal/mol range of 80.5−90.1 kcal/mol among the flavonoids. Several of the most commonly observed glycosylation patterns on tricin were also compared, including glucose or arabinose, which revealed that sugars found at the 5-O, 6-O, 7-O, and 8-O positions on tricin did not affect hydroxyl bond strength. These data suggest that radical

Table 4. Hydroxyl Bond BDEs (kcal/mol) of Flavonoids and Monolignols

monolignols					
coumaryl	caffeyl	5HG	coniferyl	ferulate	sinapyl
85.7	86.7	78.6	86.1	87.0	82.0

flavanols			
catechin (R,S)	catechin (S,R)	epicatechin (R,R)	epicatechin (S,S)
88.5	88.5	87.8	87.7
epigallocatechin	epigallocatechin gallate		
80.5	81.6		

flavones			
tricin	apigenin	luteolin	chrysoeriol
84.4	90.1	89.2	81.0

glycosylated tricins			
tricin-7-O-Glc	tricin-5-O-Glc	tricin-6-Ara-8-Glc	tricin-6-Glc-8-Ara
83.8	83.4	84.2	84.5

https://dx.doi.org/10.1021/acssuschemeng.0c04240
ACS Sustainable Chem. Eng. XXXX, XXX, XXX−XXX

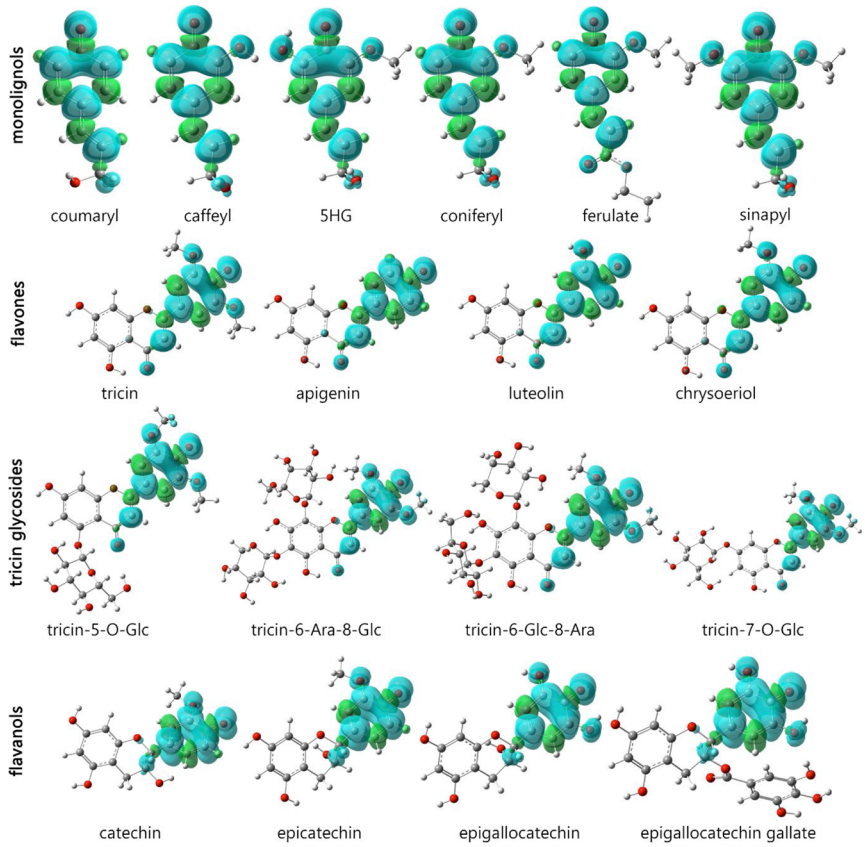

Figure 5. Spin density difference maps of activated radical monolignols and flavonoid monomers. Isosurface value = 0.001, generated in CubeGen.

activation of flavones, flavanols, and monolignols is comparably an endothermic preliminary step in lignin biosynthesis.

Spin density difference calculations have been successfully employed to depict the delocalization of the unpaired electron, revealing the reactive sites on monolignols for radical coupling in lignin polymerization.[53,78] Therefore, the density difference maps of the six monolignols and the flavonoid monomers were compared, as shown in Figure 5. In monolignols, π-electron delocalization extends beyond the conjugated ring, with particularly high spin density located on the Cβ, representative of the ability of monolignols to couple at multiple sites. Analogous to the observations of dimer linkage properties, methoxyl or hydroxyl substituents *ortho* to the site of bond cleavage most strongly impacted the 4′-OH bond strength and spin density maps. In flavonoids, delocalization beyond the phenyl ring is also observed yet to differing degrees in the flavones versus flavanols. In the flavones, unpaired electron density is seen on the C2, C3, and carbonyl groups on account of the more extended π-conjugation. In the flavanols, these carbon positions are sp^3-hybridized stereocenters and accordingly do not participate in the delocalized π-bond network, restricting the unpaired electron density to the phenyl-prime ring. These electron density differences may affect the relative radical scavenging reactivity of the different flavonoid classes due to the slightly greater radical character at the 4′-O position of flavanols.

Not explicitly seen in the maps is the additional possible coupling reactivity in epigallocatechin and epigallocatechin gallate. Due to the presence of 3′- and 5′-hydroxyl groups present both on the phenyl-prime ring and the gallate moiety, the epigallocatechins could form either 4′-O-β or benzodioxane linkages at two phenyl 4-OH sites within the flavanol. In C-lignin polymerization, experimental and theoretical works support that the formation of a benzodioxane linkage is driven by kinetic factors,[16,27] which could similarly drive intramolecular ring closure in linkages for these flavanols and have chemical implications for depolymerization. Also, unique to the epigallocatechin gallate is the presence of the two chemically similar sites for hydrogen abstraction—the 4′-OH and gallate hydroxyl—which could result in the bidirectional growth of a seeded lignin oligomer, provided that each site may be sequentially activated. With the exception of epigallocatechin gallates that may offer multiple coupling sites, the remaining flavonoids could serve as not only initiation sites but also chain terminators. These antioxidant radical scavengers could conceivably couple at their 4′-OH position with the β-O of a growing lignin chain and terminate the lignification reaction, thus imparting a dual mechanism of polymer molecular weight reduction. Further investigations could compare the coupling energetics of chain termination and help elucidate additional possible coupling reactivity of flavonoids.

On account of their additional available coupling sites, the flavonoids apigenin, luteolin, and chrysoeriol could potentially form condensed linkages β-5′ linkages or 5−5′-linkages, in contrast to tricin, in which the proximal 3′ and 5′ methoxyl groups would inhibit this reactivity. This type of linkage between canonical monolignols has been examined both theoretically[14,47] and experimentally,[19,22,70] yet these linkages with flavones remain to be investigated. Particularly, NMR studies to reveal whether such bonds with these tricin precursors are formed *in vivo* would be of significance to

https://dx.doi.org/10.1021/acssuschemeng.0c04240
ACS Sustainable Chem. Eng. XXXX, XXX, XXX−XXX

depolymerization chemistry due to these higher energy bonds contributing to lignin recalcitrance.

Many remaining unknowns about lignin chain initiation motivate future experimental works, foremost being to reveal the effects of increased flavonoid expression on the lignin oligomer weight by comparing the molecular weight distributions of tricin-overexpression lines versus wild-type plants. Additional *in vitro* studies could also clarify which flavonoid classes natively serve as initiation sites, the roles of different flavonoids and their substituent modifications, and the degree of plasticity to utilize non-native initiation sites. While tricin is the most studied flavonoid incorporated into lignin, recent experiments indicate that tricin is neither an obligatory chain initiator nor the only initiation site for lignin biosynthesis.[79] For example, in tricin knockout models, plants produced lignin with an altered monolignol content and incorporated naringenin, the precursor to flavone synthesis.[80] Therefore, the precursors just downstream from naringenin in the tricin biosynthetic pathway, apigenin, luteolin, and chrysoeriol,[57] could potentially serve as additional, alternative initiation sites. Also, other classes of flavonoids that are naturally synthesized in plants have been shown to couple to lignin.[14] As such, flavanols are likely candidates as alternatives or supplemental initiation sites and the present findings support that flavanols exhibit chemically similar H-abstraction energies and linkages to monolignols. Engineering efforts to overexpress flavanols, therefore, hinge upon experimental verification of their role as initiators and further clarifications of interdependencies between lignin composition and the type of initiator.

CONCLUSIONS

Overexpression of initiation sites to the reduce lignin molecular weight offers a promising strategy to improve the lignin depolymerization efficiency. The enriched flavonoid content in lignin would increase the significance of flavonoid-monolignol linkage strengths, which were accordingly characterized in this DFT study. BDE analyses indicate that flavonoid-monolignol 4′-O-β linkages have strengths and properties similar to inter-monolignol β-O-4 bonds. Incorporation of oxidized monolignols most significantly reduced linkage strength, with the lowest 4′-O-β strength of 53.9 kcal/mol found for F_{sat}-epigallocatechin. Flavone-monolignol dimers, however, resulted in more consistent low linkage strengths than the flavanols considered. Substituents *ortho* to the linkage more significantly affected the 4′-O-β bond strength, compared to minimal substituent effects further from the 4′-O, which was also seen for the monomer hydroxyl BDEs. Based on all enthalpy analyses conducted, we speculate that the increased incorporation of either flavones or flavanols would not be hindered by thermodynamic barriers. In whole, results support that overexpression of flavonoid initiation sites and oxidized monolignols could facilitate the production of less recalcitrant lignin oligomers.

ASSOCIATED CONTENT

Supporting Information

The Supporting Information is available free of charge at https://pubs.acs.org/doi/10.1021/acssuschemeng.0c04240.

BDEs of flavonoid-monolignol dimers, correlation of stereoisomer enthalpy with stereoisomer bond dissociation enthalpy, and final optimized coordinates of flavonoid and monolignol monomers and dimers (PDF)

AUTHOR INFORMATION

Corresponding Authors

Michael Crowley − *Renewable Resources and Enabling Sciences Center, National Renewable Energy Laboratory, Golden, Colorado 80401, United States;* orcid.org/0000-0001-5163-9398; Email: Michael.Crowley@nrel.gov

Gregg T. Beckham − *Renewable Resources and Enabling Sciences Center, National Renewable Energy Laboratory, Golden, Colorado 80401, United States;* orcid.org/0000-0002-3480-212X; Email: Gregg.Beckham@nrel.gov

Authors

Laura Berstis − *Biosciences Center, National Renewable Energy Laboratory, Golden, Colorado 80401, United States*

Thomas Elder − *USDA-Forest Service, Auburn, Alabama 36849, United States;* orcid.org/0000-0003-3909-2152

Richard Dixon − *BioDiscovery Institute and Department of Biological Sciences, University of North Texas, Denton, Texas 76203, United States;* orcid.org/0000-0001-8393-9408

Complete contact information is available at: https://pubs.acs.org/10.1021/acssuschemeng.0c04240

Notes

The authors declare no competing financial interest.

ACKNOWLEDGMENTS

This work was authored in part by the National Renewable Energy Laboratory, operated by the Alliance for Sustainable Energy, LLC, for the U.S. Department of Energy (DOE) under contract no. DE-AC36-08GO28308. L.B., M.C., and G.T.B. thank the U.S. DOE, Office of Energy Efficiency and Renewable Energy, and Bioenergy Technologies Office for funding. R.A.D. and G.T.B. also acknowledge funding from the Center for Bioenergy Innovation, a U.S. DOE Bioenergy Research Center supported by the Office of Biological and Environmental Research in the DOE Office of Science. The authors are grateful for the supercomputer time on Stampede provided by the Texas Advanced Computing Center (TACC) at the University of Texas at Austin through TG-MCB090159 and the use of the NREL Computational Sciences Center, supercomputing resource Peregrine, which is supported by the DOE Office of EERE under contract no. DE-AC36-08GO28308. This work was also made possible in part by a grant of high-performance computing resources and technical support from the Alabama Supercomputer Authority. The views expressed in the article do not necessarily represent the views of the DOE or the U.S. Government. The U.S. Government retains and the publisher, by accepting the article for publication, acknowledges that the U.S. Government retains a nonexclusive, paid-up, irrevocable, worldwide license to publish or reproduce the published form of this work, or allow others to do so, for U.S. Government purposes.

ABBREVIATIONS

BDE	bond dissociation enthalpy
C	caffeyl alcohol
DFT	density functional theory
F	ferulate

F_{sat}	ferulate in dimers with a saturated Cα−Cβ bond
G	coniferyl alcohol
H	hydroxyphenyl alcohol
S	sinapyl alcohol
5HG	5-hydroxyconiferyl alcohol

REFERENCES

(1) Himmel, M. E.; Ding, S.-Y.; Johnson, D. K.; Adney, W. S.; Nimlos, M. R.; Brady, J. W.; Foust, T. D. Biomass recalcitrance: engineering plants and enzymes for biofuels production. *Science* **2007**, *315*, 804−807.

(2) Ragauskas, A. J.; Beckham, G. T.; Biddy, M. J.; Chandra, R.; Chen, F.; Davis, M. F.; Davison, B. H.; Dixon, R. A.; Gilna, P.; Keller, M.; Langan, P.; Naskar, A. K.; Saddler, J. N.; Tschaplinski, T. J.; Tuskan, G. A.; Wyman, C. E. Lignin valorization: improving lignin processing in the biorefinery. *Science* **2014**, *344*, 1246843.

(3) Kai, D.; Tan, M. J.; Chee, P. L.; Chua, Y. K.; Yap, Y. L.; Loh, X. J. Towards lignin-based functional materials in a sustainable world. *Green Chem.* **2016**, *18*, 1175−1200.

(4) Linger, J. G.; Vardon, D. R.; Guarnieri, M. T.; Karp, E. M.; Hunsinger, G. B.; Franden, M. A.; Johnson, C. W.; Chupka, G.; Strathmann, T. J.; Pienkos, P. T.; Beckham, G. T. Lignin valorization through integrated biological funneling and chemical catalysis. *Proc. Natl. Acad. Sci. U.S.A.* **2014**, *111*, 12013−12018.

(5) Davis, R.; Tao, L.; Tan, E. C. D.; Biddy, M. J.; Beckham, G. T.; Scarlata, C.; Jacobson, J.; Cafferty, K.; Ross, J.; Lukas, J.; Knorr, D.; Schoen, P. *Process design and economics for the conversion of lignocellulosic biomass to hydrocarbons: dilute-acid and enzymatic deconstruction of biomass to sugars and biological conversion of sugars to hydrocarbons*; United States, 2013.

(6) Davis, R. E.; Grundl, N. J.; Tao, L.; Biddy, M. J.; Tan, E. C.; Beckham, G. T.; Humbird, D.; Thompson, D. N.; Roni, M. S. *Process design and economics for the conversion of lignocellulosic biomass to hydrocarbon fuels and coproducts: 2018 biochemical design case update; biochemical deconstruction and conversion of biomass to fuels and products via integrated biorefinery pathways*; United States, 2018.

(7) Corona, A.; Biddy, M. J.; Vardon, D. R.; Birkved, M.; Hauschild, M. Z.; Beckham, G. T. Life cycle assessment of adipic acid production from lignin. *Green Chem.* **2018**, *20*, 3857−3866.

(8) Rinaldi, R.; Jastrzebski, R.; Clough, M. T.; Ralph, J.; Kennema, M.; Bruijnincx, P. C. A.; Weckhuysen, B. M. Paving the way for lignin valorisation: recent advances in bioengineering, biorefining and catalysis. *Angew. Chem., Int. Ed.* **2016**, *55*, 8164−8215.

(9) Barros, J.; Serk, H.; Granlund, I.; Pesquet, E. The cell biology of lignification in higher plants. *Ann. Bot.* **2015**, *115*, 1053−1074.

(10) Boerjan, W.; Ralph, J.; Baucher, M. Lignin biosynthesis. *Annu. Rev. Plant Biol.* **2003**, *54*, 519−546.

(11) Zakzeski, J.; Bruijnincx, P. C. A.; Jongerius, A. L.; Weckhuysen, B. M. The catalytic valorization of lignin for the production of renewable chemicals. *Chem. Rev.* **2010**, *110*, 3552−3599.

(12) Schutyser, W.; Renders, T.; Van den Bosch, S.; Koelewijn, S.-F.; Beckham, G. T.; Sels, B. F. Chemicals from lignin: an interplay of lignocellulose fractionation, depolymerisation, and upgrading. *Chem. Soc. Rev.* **2018**, *47*, 852−908.

(13) Sun, Z.; Fridrich, B.; de Santi, A.; Elangovan, S.; Barta, K. Bright side of lignin depolymerization: toward new platform chemicals. *Chem. Rev.* **2018**, *118*, 614−678.

(14) del Río, J. C.; Rencoret, J.; Gutiérrez, A.; Elder, T.; Kim, H.; Ralph, J. Lignin monomers from beyond the canonical monolignol biosynthetic pathway: another brick in the wall. *ACS Sustainable Chem. Eng.* **2020**, *8*, 4997−5012.

(15) Mottiar, Y.; Vanholme, R.; Boerjan, W.; Ralph, J.; Mansfield, S. D. Designer lignins: harnessing the plasticity of lignification. *Curr. Opin. Biotechnol.* **2016**, *37*, 190−200.

(16) Chen, F.; Tobimatsu, Y.; Havkin-Frenkel, D.; Dixon, R. A.; Ralph, J. A polymer of caffeyl alcohol in plant seeds. *Proc. Natl. Acad. Sci. U.S.A.* **2012**, *109*, 1772−1777.

(17) Chen, F.; Tobimatsu, Y.; Jackson, L.; Nakashima, J.; Ralph, J.; Dixon, R. A. Novel seed coat lignins in the Cactaceae: structure, distribution and implications for the evolution of lignin diversity. *Plant J.* **2013**, *73*, 201−211.

(18) Lu, F.; Marita, J. M.; Lapierre, C.; Jouanin, L.; Morreel, K.; Boerjan, W.; Ralph, J. Sequencing around 5-hydroxyconiferyl alcohol-derived units in caffeic acid o-methyltransferase-deficient poplar lignins. *Plant Physiol.* **2010**, *153*, 569−579.

(19) Ralph, J. Hydroxycinnamates in lignification. *Phytochem. Rev.* **2009**, *9*, 65−83.

(20) Mahon, E. L.; Mansfield, S. D. Tailor-made trees: engineering lignin for ease of processing and tomorrow's bioeconomy. *Curr. Opin. Biotechnol.* **2019**, *56*, 147−155.

(21) Oyarce, P.; De Meester, B.; Fonseca, F.; de Vries, L.; Goeminne, G.; Pallidis, A.; De Rycke, R.; Tsuji, Y.; Li, Y.; Van den Bosch, S.; Sels, B.; Ralph, J.; Vanholme, R.; Boerjan, W. Introducing curcumin biosynthesis in Arabidopsis enhances lignocellulosic biomass processing. *Nat. Plants* **2019**, *5*, 225−237.

(22) Lan, W.; Rencoret, J.; Carlos del Rio, J.; Ralph, J. Tricin in grass lignin: Biosynthesis, Characterization, and Quantification. In *Lignin: Biosynthesis, Functions and Economic Significance*; Lu, F., Yue, F., Eds.; Nova Science Publishers, Inc.: 2019; Chapter 3, pp 51−78.

(23) Ralph, J.; Lapierre, C.; Boerjan, W. Lignin structure and its engineering. *Curr. Opin. Biotechnol.* **2019**, *56*, 240−249.

(24) Holwerda, E. K.; Worthen, R. S.; Kothari, N.; Lasky, R. C.; Davison, B. H.; Fu, C.; Wang, Z.-Y.; Dixon, R. A.; Biswal, A. K.; Mohnen, D.; Nelson, R. S.; Baxter, H. L.; Mazarei, M.; Stewart, C. N.; Muchero, W.; Tuskan, G. A.; Cai, C. M.; Gjersing, E. E.; Davis, M. F.; Himmel, M. E.; Wyman, C. E.; Gilna, P.; Lynd, L. R. Multiple levers for overcoming the recalcitrance of lignocellulosic biomass. *Biotechnol. Biofuels* **2019**, *12*, 1−12.

(25) Bonawitz, N. D.; Chapple, C. The genetics of lignin biosynthesis: connecting genotype to phenotype. *Annu. Rev. Genet.* **2010**, *44*, 337−363.

(26) Tobimatsu, Y.; Schuetz, M. Lignin polymerization: how do plants manage the chemistry so well? *Curr. Opin. Biotechnol.* **2019**, *56*, 75−81.

(27) Berstis, L.; Elder, T.; Crowley, M.; Beckham, G. T. Radical nature of c-lignin. *ACS Sustainable Chem. Eng.* **2016**, *4*, 5327−5335.

(28) Stewart, J. J.; Akiyama, T.; Chapple, C.; Ralph, J.; Mansfield, S. D. The effects on lignin structure of overexpression of ferulate 5-hydroxylase in hybrid poplar. *Plant Physiol.* **2009**, *150*, 621−635.

(29) Wilkerson, C. G.; Mansfield, S. D.; Lu, F.; Withers, S.; Park, J.-Y.; Karlen, S. D.; Gonzales-Vigil, E.; Padmakshan, D.; Unda, F.; Rencoret, J.; Ralph, J. Monolignol ferulate transferase introduces chemically labile linkages into the lignin backbone. *Science* **2014**, *344*, 90−93.

(30) Zhou, S.; Runge, T.; Karlen, S. D.; Ralph, J.; Gonzales-Vigil, E.; Mansfield, S. D. Chemical pulping advantages of zip-lignin hybrid poplar. *ChemSusChem* **2017**, *10*, 3565−3573.

(31) Tuskan, G. A. The unexpected malleability of lignin. *Nat. Plants* **2019**, *5*, 128.

(32) Bonawitz, N. D.; Kim, J. I.; Tobimatsu, Y.; Ciesielski, P. N.; Anderson, N. A.; Ximenes, E.; Maeda, J.; Ralph, J.; Donohoe, B. S.; Ladisch, M.; Chapple, C. Disruption of Mediator rescues the stunted growth of a lignin-deficient Arabidopsis mutant. *Nature* **2014**, *509*, 376−380.

(33) Eudes, A.; Liang, Y.; Mitra, P.; Loqué, D. Lignin bioengineering. *Curr. Opin. Biotechnol.* **2014**, *26*, 189−198.

(34) Syrjänen, K.; Brunow, G. Oxidative cross coupling of p-hydroxycinnamic alcohols with dimeric arylglycerol β-aryl ether lignin model compounds. The effect of oxidation potentials. *J. Chem. Soc., Perkin Trans. 1* **1998**, 3425−3430.

(35) Vanholme, R.; Morreel, K.; Darrah, C.; Oyarce, P.; Grabber, J. H.; Ralph, J.; Boerjan, W. Metabolic engineering of novel lignin in biomass crops. *New Phytol.* **2012**, *196*, 978−1000.

(36) Eudes, A.; George, A.; Mukerjee, P.; Kim, J. S.; Pollet, B.; Benke, P. I.; Yang, F.; Mitra, P.; Sun, L.; Çetinkol, Ö. P.; Chabout, S.; Mouille, G.; Soubigou-Taconnat, L.; Balzergue, S.; Singh, S.; Holmes,

https://dx.doi.org/10.1021/acssuschemeng.0c04240
ACS Sustainable Chem. Eng. XXXX, XXX, XXX−XXX

B. M.; Mukhopadhyay, A.; Keasling, J. D.; Simmons, B. A.; Lapierre, C.; Ralph, J.; Loqué, D. Biosynthesis and incorporation of side-chain-truncated lignin monomers to reduce lignin polymerization and enhance saccharification. *Plant Biotechnol. J.* **2012**, *10*, 609−620.
(37) del Río, J. C.; Rencoret, J.; Prinsen, P.; Martínez, Á. T.; Ralph, J.; Gutiérrez, A. Structural characterization of wheat straw lignin as revealed by analytical pyrolysis, 2D-NMR, and reductive cleavage methods. *J. Agric. Food Chem.* **2012**, *60*, 5922−5935.
(38) Lan, W.; Lu, F.; Regner, M.; Zhu, Y.; Rencoret, J.; Ralph, S. A.; Zakai, U. I.; Morreel, K.; Boerjan, W.; Ralph, J. Tricin, a flavonoid monomer in monocot lignification. *Plant Physiol.* **2015**, *167*, 1284−1295.
(39) Lan, W.; Morreel, K.; Lu, F.; Rencoret, J.; del Río, J. C.; Voorend, W.; Vermerris, W.; Boerjan, W. A.; Ralph, J. Maize tricin-oligolignol metabolites and their implications for monocot lignification. *Plant Physiol.* **2016**, *171*, 810−820.
(40) Li, M.; Pu, Y.; Yoo, C. G.; Ragauskas, A. J. The occurrence of tricin and its derivatives in plants. *Green Chem.* **2016**, *18*, 1439−1454.
(41) García-Lafuente, A.; Guillamón, E.; Villares, A.; Rostagno, M. A.; Martínez, J. A. Flavonoids as anti-inflammatory agents: implications in cancer and cardiovascular disease. *Inflammation Res.* **2009**, *58*, 537−552.
(42) Oyama, T.; Yasui, Y.; Sugie, S.; Koketsu, M.; Watanabe, K.; Tanaka, T. Dietary tricin suppresses inflammation-related colon carcinogenesis in male crj: CD-1 mice. *Cancer Prev. Res.* **2009**, *2*, 1031−1038.
(43) Ajitha, M. J.; Mohanlal, S.; Suresh, C. H.; Jayalekshmy, A. DPPH radical scavenging activity of tricin and its conjugates isolated from "njavara" rice bran: a density functional theory study. *J. Agric. Food Chem.* **2012**, *60*, 3693−3699.
(44) Grabber, J. H.; Schatz, P. F.; Kim, H.; Lu, F.; Ralph, J. Identifying new lignin bioengineering targets: 1. Monolignol-substitute impacts on lignin formation and cell wall fermentability. *BMC Plant Biol.* **2010**, *10*, 114.
(45) Iñiguez-Franco, F.; Soto-Valdez, H.; Peralta, E.; Ayala-Zavala, J. F.; Auras, R.; Gámez-Meza, N. Antioxidant activity and diffusion of catechin and epicatechin from antioxidant active films made of poly(l-lactic acid). *J. Agric. Food Chem.* **2012**, *60*, 6515−6523.
(46) Mouradov, A.; Spangenberg, G. Flavonoids: a metabolic network mediating plants adaptation to their real estate. *Front. Plant Sci.* **2014**, *5*, 620.
(47) Elder, T. Bond dissociation enthalpies of a pinoresinol lignin model compound. *Energy Fuels* **2014**, *28*, 1175−1182.
(48) Lan, W.; Rencoret, J.; Lu, F.; Karlen, S. D.; Smith, B. G.; Harris, P. J.; del Río, J. C.; Ralph, J. Tricin-lignins: occurrence and quantitation of tricin in relation to phylogeny. *Plant J.* **2016**, *88*, 1046−1057.
(49) Aaboer, D. B. F.; Bleeg, I. S.; Christensen, B. T.; Kondo, T.; Brandt, K. Flavone c-glycoside, phenolic acid, and nitrogen contents in leaves of barley subject to organic fertilization treatments. *J. Agric. Food Chem.* **2003**, *51*, 809−813.
(50) Elder, T. Bond dissociation enthalpies of a dibenzodioxocin lignin model compound. *Energy Fuels* **2013**, *27*, 4785−4790.
(51) Kim, S.; Chmely, S. C.; Nimlos, M. R.; Bomble, Y. J.; Foust, T. D.; Paton, R. S.; Beckham, G. T. Computational study of bond dissociation enthalpies for a large range of native and modified lignins. *J. Phys. Chem. Lett.* **2011**, *2*, 2846−2852.
(52) Sangha, A. K.; Davison, B. H.; Standaert, R. F.; Davis, M. F.; Smith, J. C.; Parks, J. M. Chemical factors that control lignin polymerization. *J. Phys. Chem. B* **2014**, *118*, 164−170.
(53) Sangha, A. K.; Parks, J. M.; Standaert, R. F.; Ziebell, A.; Davis, M.; Smith, J. C. Radical coupling reactions in lignin synthesis: a density functional theory study. *J. Phys. Chem. B* **2012**, *116*, 4760−4768.
(54) Beste, A.; Buchanan, A. C. Computational study of bond dissociation enthalpies for lignin model compounds. Substituent effects in phenethyl phenyl ethers. *J. Org. Chem.* **2009**, *74*, 2837−2841.
(55) Younker, J. M.; Beste, A.; Buchanan, A. C. Computational study of bond dissociation enthalpies for substituted β-O-4 lignin model compounds. *ChemPhysChem* **2011**, *12*, 3556−3565.
(56) Younker, J. M.; Beste, A.; Buchanan, A. C. Computational study of bond dissociation enthalpies for lignin model compounds: β-5 Arylcoumaran. *Chem. Phys. Lett.* **2012**, *545*, 100−106.
(57) Lam, P. Y.; Liu, H.; Lo, C. Completion of tricin biosynthesis pathway in rice: cytochrome p450 75b4 is a unique chrysoeriol 5′-hydroxylase. *Plant Physiol.* **2015**, *168*, 1527−1536.
(58) Frisch, M. J.; Trucks, G. W.; Schlegel, H. B.; Scuseria, G. E.; Robb, M. A.; Cheeseman, J. R.; Scalmani, G.; Barone, V.; Petersson, G. A.; Nakatsuji, H.; Li, X.; Caricato, M.; Marenich, A.; Bloino, J.; Janesko, B. G.; Gomperts, R.; Mennucci, B.; Hratchian, H. P.; Ortiz, J. V.; Izmaylov, A. F.; Sonnenberg, J. L.; Williams-Young, D.; Ding, F.; Lipparini, F.; Egidi, F.; Goings, J.; Peng, B.; Petrone, A.; Henderson, T.; Ranasinghe, D.; Zakrzewski, V. G.; Gao, J.; Rega, N.; Zheng, G.; Liang, W.; Hada, M.; Ehara, M.; Toyota, K.; Fukuda, R.; Hasegawa, J.; Ishida, M.; Nakajima, T.; Honda, Y.; Kitao, O.; Nakai, H.; Vreven, T.; Throssell, K.; Montgomery, J. A., Jr.; Peralta, J. E.; Ogliaro, F.; Bearpark, M.; Heyd, J. J.; Brothers, E.; Kudin, K. N.; Staroverov, V. N.; Keith, T.; Kobayashi, R.; Normand, J.; Raghavachari, K.; Rendell, A.; Burant, J. C.; Iyengar, S. S.; Tomasi, J.; Cossi, M.; Millam, J. M.; Klene, M.; Adamo, C.; Cammi, R.; Ochterski, J. W.; Martin, R. L.; Morokuma, K.; Farkas, O.; Foresman, J. B.; Fox, D. J. *Gaussian09*; Gaussian, Inc.: Wallingford, CT, USA, 2009.
(59) Ponder, J. W.; Richards, F. M. An efficient Newton-like method for molecular mechanics energy minimization of large molecules. *J. Comput. Chem.* **1987**, *8*, 1016−1024.
(60) Halgren, T. A. Merck molecular force field. I. Basis, form, scope, parameterization, and performance of MMFF94. *J. Comput. Chem.* **1996**, *17*, 490−519.
(61) Elder, T.; Berstis, L.; Beckham, G. T.; Crowley, M. F. Coupling and reactions of 5-hydroxyconiferyl alcohol in lignin formation. *J. Agric. Food Chem.* **2016**, *64*, 4742−4750.
(62) MOPAC2009; Stewart, J. J. P. *Stewart Computational Chemistry*; Colorado Springs: CO, USA, 2008.
(63) Hohenstein, E. G.; Chill, S. T.; Sherrill, C. D. Assessment of the performance of the M05−2X and M06−2X exchange-correlation functionals for noncovalent interactions in biomolecules. *J. Chem. Theory Comput.* **2008**, *4*, 1996−2000.
(64) Zhao, Y.; Truhlar, D. G. The M06 suite of density functionals for main group thermochemistry, thermochemical kinetics, noncovalent interactions, excited states, and transition elements: two new functionals and systematic testing of four M06-class functionals and 12 other functionals. *Theor. Chem. Acc.* **2007**, *120*, 215−241.
(65) Zhao, Y.; Truhlar, D. G. Applications and validations of the Minnesota density functionals. *Chem. Phys. Lett.* **2011**, *502*, 1−13.
(66) Weigend, F.; Ahlrichs, R. Balanced basis sets of split valence, triple zeta valence and quadruple zeta valence quality for H to Rn: Design and assessment of accuracy. *Phys. Chem. Chem. Phys.* **2005**, *7*, 3297−3305.
(67) Lange, H.; Decina, S.; Crestini, C. Oxidative upgrade of lignin − Recent routes reviewed. *Eur. Polym. J.* **2013**, *49*, 1151−1173.
(68) Rahimi, A.; Ulbrich, A.; Coon, J. J.; Stahl, S. S. Formic-acid-induced depolymerization of oxidized lignin to aromatics. *Nature* **2014**, *515*, 249−252.
(69) Li, M.; Pu, Y.; Ragauskas, A. J. Current understanding of the correlation of lignin structure with biomass recalcitrance. *Front. Chem.* **2016**, *4*, 45.
(70) Lan, W.; Yue, F.; Rencoret, J.; del Río, J.; Boerjan, W.; Lu, F.; Ralph, J. Elucidating tricin-lignin structures: assigning correlations in HSQC spectra of monocot lignins. *Polymers* **2018**, *10*, 916.
(71) Elder, T.; Berstis, L.; Beckham, G. T.; Crowley, M. F. Coupling and reactions of 5-hydroxyconiferyl alcohol in lignin formation. *J. Agric. Food Chem.* **2016**, *64*, 4742−4750.
(72) Martinez, C. R.; Iverson, B. L. Rethinking the term "pi-stacking". *Chem. Sci.* **2012**, *3*, 2191−2201.

https://dx.doi.org/10.1021/acssuschemeng.0c04240
ACS Sustainable Chem. Eng. XXXX, XXX, XXX−XXX

(73) Zhao, R.; Zhang, R.-Q. A new insight into $\pi-\pi$ stacking involving remarkable orbital interactions. *Phys. Chem. Chem. Phys.* **2016**, *18*, 25452−25457.
(74) Mishra, P. K.; Ekielski, A. The self-assembly of lignin and its application in nanoparticle synthesis: a short review. *Nanomaterials* **2019**, *9*, 243.
(75) Bartzoka, E. D.; Lange, H.; Thiel, K.; Crestini, C. Coordination complexes and one-step assembly of lignin for versatile nanocapsule engineering. *ACS Sustainable Chem. Eng.* **2016**, *4*, 5194−5203.
(76) Bartzoka, E. D.; Lange, H.; Mosesso, P.; Crestini, C. Synthesis of nano- and microstructures from proanthocyanidins, tannic acid and epigallocatechin-3-O-gallate for active delivery. *Green Chem.* **2017**, *19*, 5074−5091.
(77) Vermaas, J. V.; Petridis, L.; Ralph, J.; Crowley, M. F.; Beckham, G. T. Systematic parameterization of lignin for the CHARMM force field. *Green Chem.* **2019**, *21*, 109−122.
(78) Elder, T.; Fort, R. C. Reactivity of Lignin—Correlation with Molecular Orbital Calculations. In *Lignin and Lignans: Advances in Chemistry*; Heitner, C., Dimmel, D. R., Schmidt, J. A.; CRC Press: Boca Raton, FL, 2010; pp 321−347.
(79) Dixon, R. A.; Barros, J. Lignin biosynthesis: old roads revisited and new roads explored. *Open Biol.* **2019**, *9*, 190215.
(80) Lam, P. Y.; Tobimatsu, Y.; Takeda, Y.; Suzuki, S.; Yamamura, M.; Umezawa, T.; Lo, C. Disrupting flavone synthase II alters lignin and improves biomass digestibility. *Plant Physiol.* **2017**, *174*, 972−985.
(81) Elder, T.; Beste, A. Density functional theory study of the concerted pyrolysis mechanism for lignin models. *Energy Fuels* **2014**, *28*, 5229−5235.
(82) Grabber, J. H.; Hatfield, R. D.; Lu, F.; Ralph, J. Coniferyl ferulate incorporation into lignin enhances the alkaline delignification and enzymatic degradation of cell walls. *Biomacromolecules* **2008**, *9*, 2510−2516.
(83) Elumalai, S.; Tobimatsu, Y.; Grabber, J. H.; Pan, X.; Ralph, J. Epigallocatechin gallate incorporation into lignin enhances the alkaline delignification and enzymatic saccharification of cell walls. *Biotechnol. Biofuels* **2012**, *5*, 59.

https://dx.doi.org/10.1021/acssuschemeng.0c04240
ACS Sustainable Chem. Eng. XXXX, XXX, XXX−XXX